

Environmental parameter estimation with the two-level atom probes

Mengmeng Luo(罗萌萌), Wenxiao Liu(刘文晓), Yuetao Chen(陈悦涛), Shangbin Han(韩尚斌), and Shaoyan Gao(高韶燕)

Citation: Chin. Phys. B, 2022, 31 (**5**): 050304. DOI: 10.1088/1674-1056/ac364f
Journal homepage: http://cpb.iphy.ac.cn; http://iopscience.iop.org/cpb

What follows is a list of articles you may be interested in

Quantum exceptional points of non-Hermitian Hamiltonian and Liouvillian in dissipative quantum Rabi model

Xianfeng Ou(欧先锋), Jiahao Huang(黄嘉豪), and Chaohong Lee(李朝红)
Chin. Phys. B, 2021, 30 (**11**): 110309. DOI: 10.1088/1674-1056/ac0349

Quantum metrology with coherent superposition of two different coded channels

Dong Xie(谢东), Chunling Xu(徐春玲), and Anmin Wang(王安民)
Chin. Phys. B, 2021, 30 (**9**): 090304. DOI: 10.1088/1674-1056/ac0bae

Optimal parameter estimation of open quantum systems

Yinghua Ji(嵇英华), Qiang Ke(柯强), and Juju Hu(胡菊菊)
Chin. Phys. B, 2020, 29 (**12**): 120303. DOI: 10.1088/1674-1056/abc0d1

Quantum metrology with a non-Markovian qubit system

Jiang Huang(黄江), Wen-Qing Shi(师文庆), Yu-Ping Xie(谢玉萍), Guo-Bao Xu(徐国保), Hui-Xian Wu(巫慧娴)
Chin. Phys. B, 2018, 27 (**12**): 120301. DOI: 10.1088/1674-1056/27/12/120301

Modulating quantum Fisher information of qubit in dissipative cavity by coupling strength

Danping Lin(林丹萍), Yu Liu(刘禹), Hong-Mei Zou(邹红梅)
Chin. Phys. B, 2018, 27 (**11**): 110303. DOI: 10.1088/1674-1056/27/11/110303

Environmental parameter estimation with the two-level atom probes

Mengmeng Luo(罗萌萌)[1], Wenxiao Liu(刘文晓)[2], Yuetao Chen(陈悦涛)[1], Shangbin Han(韩尚斌)[1], and Shaoyan Gao(高韶燕)[1,†]

[1] *MOE Key Laboratory for Nonequilibrium Synthesis and Modulation of Condensed Matter, Shaanxi Province Key Laboratory of Quantum Information and Quantum Optoelectronic Devices, School of Physics, Xi'an Jiaotong University, Xi'an* 710049, *China*

[2] *Department of Physics and Electronics, North China University of Water Resources and Electric Power, Zhengzhou* 450046, *China*

(Received 16 August 2021; revised manuscript received 29 October 2021; accepted manuscript online 4 November 2021)

A novel scheme is proposed to estimate three environmental parameters, the detuning, the temperature and the squeezing strength with one-qubit or two-qubit probes. Quantum Fisher information and the fidelity of the atom probes are calculated. When the detuning between the frequency of cavity field and the atomic transition frequency is estimated, the dynamics of quantum Fisher information shows oscillatory and rising behaviors. To estimate the temperature of the thermal reservoir, the one-qubit probe with the superposition initial state is more favorable than the two-qubit probe with the entangled initial state. When the squeezing strength of the squeezed vacuum reservoir is estimated, we find that the estimation precision is significantly improved by utilizing the two-qubit probe with the maximal entangled initial state. Our work provides a potential application in the open quantum system and quantum information processing.

Keywords: quantum parameter estimation, quantum Fisher information, Jaynes–Cummings model, quantum reservoir theory

PACS: 03.67.–a, 06.20.–f, 42.50.Pq, 03.65.Ud **DOI:** 10.1088/1674-1056/ac364f

1. Introduction

During the past decades, quantum parameter estimation has attracted increasing attention of researchers to the issues of quantum metrology and quantum information processing. Quantum Fisher information (QFI), used to evaluate the accuracy limits of quantum measurements, plays an important role in quantum parameter estimation. QFI has been widely applied in theoretical and experimental physics, including estimating the phase and frequency,[1–19] quantifying quantum coherence[20] and recognizing multi-particle entanglement.[21,22] Besides, QFI is also applied in biology.[23] It is universally accepted that entangled states can achieve a better precision than unentangled ones.[24–29] However, some studies indicate that not all entangled states are helpful for quantum metrology.[30,31] In reality, the estimation precision of the parameters is unavoidably affected by its environment, and several schemes were proposed to protect the QFI in the structured reservoir, such as using quantum screening,[32] driving multi-particle systems,[33] optimizing the controllable parameters,[34] and combing no-knowledge quantum feedback control with quantum weak measurement.[35] The environment is often complex. Thus, it is difficult to directly obtain the information of the environment parameters. Due to the tiny perturbance, quantum sensing technique with the use of quantum probe has been developed to indirectly extract the information of the environment parameters after the probes interact with the system.

When the atom interacts with the field, many quantum phenomena are affected by the detuning between the atomic transition frequency and the frequency of cavity field, such as the population difference between two atomic levels, the quantum statistical properties of the radiation field and the atomic squeezing effects. Consequently, improving the precision of the detuning is one of the important subjects in quantum metrology. Some researchers have investigated the estimation of the detuning via QFI. Gammelmark *et al.* estimated the detuning, the Rabi frequency and the decay rate of the atom in open quantum systems.[36] Kiilerich *et al.* showed the detuning estimation in a laser-driven Λ-type atom by multichannel photon counting.[37] Dimani *et al.* found that optimized states compared with multiple single-photon states and NOON states could improve the precision of the detuning estimation over the standard quantum limit.[38] Most recently, Mogilevtsev *et al.* demonstrated that the Heisenberg limit can be restored when the detuning is estimated in the N two-level systems coupled with a single bosonic dephasing reservoir.[39] But it is difficult to realize the probe states or the detection methods of the above schemes in the experiment. As another important parameter of the environment, temperature is one of the seven fundamental physical quantities. At present, many schemes have been proposed to improve the estimation precision of the temperature with quantum estimation theory, such as a ring-structure system interacting with the bath,[40] two-level atoms transported through an optical cavity,[41] a uniformly accelerated two-level atom coupled to a massless scalar field in the Minkowski vacuum,[42] and the probe system embedded into the structured reservoir.[43–47] However, the model that the two-level system (qubit) is directly immersed in a ther-

†Corresponding author. E-mail: gaosy@xjtu.edu.cn

© 2022 Chinese Physical Society and IOP Publishing Ltd

mal reservoir has not been utilized for the temperature estimation. In addition, several researchers have reported that the squeezed state or reservoir has the potential to protect the nonclassical effects of the quantum system[48] and improve the accuracy of phase estimation.[49–53] There are many studies on estimating the squeezing strength of the squeezed state by Gaussian probes,[54–61] but little attention has been paid to estimating the squeezing strength of the squeezed vacuum reservoir. The information of the environmental parameters can be obtained by the two-level atomic system which is always considered as the quantum information carrier. The properties of the atom will be influenced by the field with a boundary, such as the Purcell effect.[62] In reality, the effects of the reservoir on the system have to be considered. Furthermore, much effort has been spent on investigating quantum effect based on the model that the atom interacts with the optical cavity, the thermal reservoir or the squeezed vacuum reservoir, respectively.

In this paper, a simple model, in which a single two-level atom couples with the Fock state field, the thermal reservoir and the squeezed vacuum reservoir, respectively, is established to calculate the QFI of the environmental parameters and the fidelity of the atom probes. Furthermore, we investigate the effects of the system parameters on the QFI and fidelity, the non-Markovian behavior, the relation between the results of the QFI and fidelity. Besides, the study is extended to the two-qubit probe with the maximally entangled initial state. The results reveal that the high-precision estimation of the detuning can be realized by employing the two-qubit probe, and the QFI of the temperature is enhanced with the increase of the interaction time under the one-qubit probe with the superposition initial state. When the squeezing strength is estimated, a drop and rise of the QFI occurs with the one-qubit probe, and the estimation precision is further enhanced by using the two-qubit probe.

The rest of this paper is organized as follows. In Section 2, parameter estimation theory is overviewed briefly in quantum systems. In Section 3, we introduce the model that the two-level atom probes are coupled to a Fock state field, a thermal reservoir, and a squeezed vacuum reservoir, respectively, and we also investigate the dynamics of the QFI and time dependence of the fidelity under different conditions. Finally, our conclusions are summarized in Section 4.

2. Parameter estimation theory

In the quantum estimation theory, the variation of a parameter ϕ can be estimated by the quantum Cramér–Rao bound,[63,64] $\delta\phi \geqslant 1/\sqrt{\nu F_{\rm Q}}$, where ν is the number of experiments and $F_{\rm Q}$ is the QFI. It is obvious that a better precision can be obtained as the value of QFI increases. Based on the density operator with spectrum decomposition under the diagonalized representation, the density matrix ρ can be written as

$$\rho = \sum_{i=1}^{N} p_i |\psi_i\rangle\langle\psi_i|, \tag{1}$$

where p_i and ψ_i are the eigenvalues and eigenvectors of ρ, respectively. The QFI can be expressed as follows:[65]

$$F_{\rm Q}(\phi) = \sum_i \frac{(\partial_\phi p_i)^2}{p_i} + 2\sum_{i\neq j}\frac{(p_i-p_j)^2}{p_i+p_j}\left|\langle\psi_i|\partial_\phi\psi_j\rangle\right|^2, \tag{2}$$

where $p_i \neq 0$ and $p_i + p_j \neq 0$.

Fidelity is usually applied to measure the degree of similarity between two quantum states. The fidelity of two quantum states is given by[66]

$$f(\rho_0,\rho_1) = {\rm tr}\sqrt{\sqrt{\rho_1}\rho_0\sqrt{\rho_1}}, \tag{3}$$

and especially, for one-qubit system, the fidelity of two quantum states can be written as

$$\begin{aligned} f(\rho_0,\rho_1) =\ & \frac{1}{2}\{1+\boldsymbol{a}_0\cdot\boldsymbol{a}_1 \\ & +[(1-\boldsymbol{a}_0\cdot\boldsymbol{a}_0)(1-\boldsymbol{a}_1\cdot\boldsymbol{a}_1)]^{1/2}\}, \end{aligned} \tag{4}$$

where $\boldsymbol{a}$ is the Bloch vector of density matrix ρ under Bloch representation. Hence, the fidelity between the initial state and final state of the atom can be obtained. In this paper, it is worth noting that $\boldsymbol{a}_0$ and $\boldsymbol{a}_1$ are the Bloch vectors of the initial atomic state and the final atomic state, respectively.

3. The model and results

In this paper, two different probe systems are considered. One is a single two-level atom, and the other is two two-level atoms.

In order to calculate the QFI of the detuning, temperature and squeezing strength, we assume the two-level system interacts with a Fock state field, a thermal reservoir and a squeezed vacuum reservoir, respectively. When the quality factor of the cavity is assumed as infinite, the atom–field interaction Hamiltonian can be written as Eq. (5a), while the atom–reservoir interaction Hamiltonian is expressed as Eq. (5b);[67]

$$H_{\rm I}' = \hbar\lambda(\sigma_+\hat{a}\,{\rm e}^{{\rm i}\Delta t} + \hat{a}^\dagger\sigma_-\,{\rm e}^{-{\rm i}\Delta t}), \tag{5a}$$

$$H_{\rm I}'' = \hbar\sum_k g_k(\sigma_+\hat{b}_k\,{\rm e}^{{\rm i}(\omega_0-\nu_k)t} + \hat{b}_k^\dagger\sigma_-\,{\rm e}^{-{\rm i}(\omega_0-\nu_k)t}), \tag{5b}$$

where Δ ($\Delta = \omega_0 - \omega$) means the detuning between the atomic transition frequency and the frequency of the cavity field, which indicates that the frequency of the cavity field can be obtained by the detuning and the atomic transition frequency. ν_k is the frequency of the k-th reservoir mode, and σ_+ (σ_-) is the rising (lowing) operator of the atom, that is, $|e\rangle\langle g|$ ($|g\rangle\langle e|$). $\hat{a}^\dagger$ ($\hat{a}$) and $\hat{b}_k^\dagger$ ($\hat{b}_k$) denote the creation (annihilation) operators of the cavity and reservoir, respectively.

When a single two-level atom interacts with a Fock state field, the initial state of the atom-field system is supposed as $|\psi_{(0)}\rangle = \cos(\alpha)|e,n\rangle + \sin(\alpha)|g,n+1\rangle$, where n means the number of photons in the cavity. The initial state is a product state when $\alpha = 0°$, while the initial state is an entangled state when $\alpha = 45°$. The initial state of the atom is prepared as $|\psi_{(0)}\rangle_{\rm A} = \cos(\alpha)|e\rangle + \sin(\alpha)|g\rangle$ when a single two-level atom interacts with the reservoir. The initial state is an eigenstate when $\alpha = 0°$, while the initial state is the superposition state when $\alpha = 45°$.

The initial atomic state is prepared in the maximal entanglement state $|\psi_{(0)}\rangle_{\rm S} = \frac{1}{\sqrt{2}}(|e_{\rm A},g_{\rm B}\rangle + |g_{\rm A},e_{\rm B}\rangle)$ when the two-qubit probe is applied, while the cavity field is initially prepared in the Fock state $\rho_{\rm f}(0) = |n\rangle\langle n|$.

When single two-level or two two-level atoms are embedded in the Fock state field, the thermal reservoir or the squeezed vacuum reservoir, respectively, the density matrix of the probe systems are calculated in the following.

3.1. The quantum estimation of the detuning in Fock state field

To begin with, the single two-level atom is coupled to a cavity with a Fock state field. In the basis $|e,n\rangle$ and $|g,n+1\rangle$, by using the schrödinger equation and tracing over the cavity field degrees of freedom, the reduced density matrix is given by[67]

$$\rho_1(t) = \begin{pmatrix} \rho_{11} & 0 \\ 0 & \rho_{22} \end{pmatrix}, \tag{6}$$

where $\rho_{11} = |\beta_1|^2$ and $\rho_{22} = |\beta_2|^2$, with

$$\begin{aligned}
\beta_1 &= {\rm e}^{{\rm i}\frac{\Delta}{2}t}\left\{\cos(\alpha)\left[\cos\left(\frac{1}{2}\widetilde{\Omega}_n t\right) - {\rm i}\frac{\Delta}{\widetilde{\Omega}_n}\sin\left(\frac{1}{2}\widetilde{\Omega}_n t\right)\right]\right. \\
&\quad \left. - {\rm i}\sin(\alpha)\frac{\Omega_n}{\widetilde{\Omega}_n}\sin\left(\frac{1}{2}\widetilde{\Omega}_n t\right)\right\}, \\
\beta_2 &= {\rm e}^{-{\rm i}\frac{\Delta}{2}t}\left\{\sin(\alpha)\left[\cos\left(\frac{1}{2}\widetilde{\Omega}_n t\right) + {\rm i}\frac{\Delta}{\widetilde{\Omega}_n}\sin\left(\frac{1}{2}\widetilde{\Omega}_n t\right)\right]\right. \\
&\quad \left. - {\rm i}\cos(\alpha)\frac{\Omega_n}{\widetilde{\Omega}_n}\sin\left(\frac{1}{2}\widetilde{\Omega}_n t\right)\right\},
\end{aligned} \tag{7}$$

while $\widetilde{\Omega}_n = \sqrt{\Omega_n^2 + \Delta^2}$ and $\Omega_n = 2\lambda\sqrt{n+1}$.

When two two-level atoms interact with the Fock state field, the wave function can be written as

$$\begin{aligned}
\psi(t) &= C_1|e_{\rm A},e_{\rm B},n-1\rangle + C_2|e_{\rm A},g_{\rm B},n\rangle \\
&\quad + C_3|g_{\rm A},e_{\rm B},n\rangle + C_4|g_{\rm A},g_{\rm B},n+1\rangle .
\end{aligned} \tag{8}$$

For simplicity, we assume the initial state of the cavity is a vacuum state, i.e., $n = 0$, and neglect the dipole–dipole interaction between the two atoms, then, the probability amplitudes are given by

$$C_1 = 0, \tag{9a}$$

$$\begin{aligned}
C_2 &= \frac{\cos(\alpha)+\sin(\alpha)}{2}\left[\cos\left(\frac{\Omega t}{2}\right) - \frac{{\rm i}\Delta}{\Omega}\sin\left(\frac{\Omega t}{2}\right)\right]{\rm e}^{{\rm i}\frac{\Delta}{2}t} \\
&\quad + \frac{\cos(\alpha)-\sin(\alpha)}{2},
\end{aligned} \tag{9b}$$

$$\begin{aligned}
C_3 &= \frac{\cos(\alpha)+\sin(\alpha)}{2}\left[\cos\left(\frac{\Omega t}{2}\right) - \frac{{\rm i}\Delta}{\Omega}\sin\left(\frac{\Omega t}{2}\right)\right]{\rm e}^{{\rm i}\frac{\Delta}{2}t} \\
&\quad + \frac{\sin(\alpha)-\cos(\alpha)}{2},
\end{aligned} \tag{9c}$$

$$C_4 = -[\cos(\alpha)+\sin(\alpha)]\frac{2{\rm i}\lambda}{\Omega}\sin\left(\frac{\Omega t}{2}\right){\rm e}^{-{\rm i}\frac{\Delta}{2}t}, \tag{9d}$$

where $\Omega = \sqrt{8\lambda^2 + \Delta^2}$. After tracing over the field, the evolved state of the system can be obtained as

$$\rho_2(t) = \begin{pmatrix} 0 & 0 & 0 & 0 \\ 0 & \rho_{22} & \rho_{23} & 0 \\ 0 & \rho_{32} & \rho_{33} & 0 \\ 0 & 0 & 0 & \rho_{44} \end{pmatrix}, \tag{10}$$

where $\rho_{22} = |C_2|^2$, $\rho_{23} = C_2C_3^*$, $\rho_{32} = C_3C_2^*$, $\rho_{33} = |C_3|^2$ and $\rho_{44} = |C_4|^2$.

Then, we obtain the QFI of the detuning by substituting the eigenvalues and eigenvectors of Eqs. (6) and (10) into Eq. (2). Note that the QFI of the estimated parameters are zero at $t = 0$, therefore, the time will start at $\lambda t = 1$ or $\gamma t = 0.1$ for calculating the QFI.

The fidelity of the atomic system can be worked out through putting the initial atomic state and the final atomic state into Eq. (3). In our scheme, the meaning of the fidelity is the closeness between the initial atomic state and the evolved atomic state.

When the probe is a single two-level atom, the QFI of the detuning is plotted in Fig. 1(a) with the product or entangled states as initial states. Figure 1(a) shows the QFI has oscillatory and rising behaviors in any initial state of the system, which means the information of the detuning flows from the probe system to the environment. From Fig. 1(a), one can conclude that a better precision of the detuning estimation can be gotten by controlling the interaction time, and the non-Markovianity appears in the periods, which indicates the existence of the memory effect. We find that the maximal QFI of the detuning estimation is 1.14×10^3 in the last period when the initial state of the system is a product state, while the maximal QFI is 1.18×10^3 when the initial state of the system is an entangled state. The best precision of the detuning estimation is obtained via substituting the value of QFI into Cramér–Rao inequality with $\nu = 1$. Although the entangled state is more advantageous to improve the precision of the detuning estimation, its result is very close to the result of the product state. Time dependence of the fidelity for the atom coupled to Fock state field is shown in Fig. 1(b). More interestingly, Fig. 1(b) also presents an oscillatory behavior and the value of the fidelity is slightly larger when the initial state of the system is

the entangled sate. From Figs. 1(a) and 1(b), one can conclude that the entangled state is more beneficial to estimating the detuning.

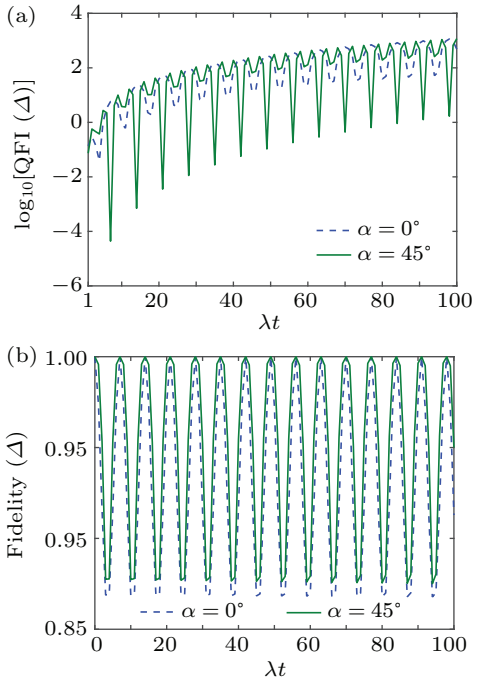


Fig. 1. When one-qubit probe is applied, (a) QFI of the detuning Δ as a function of time for different α, $\alpha = 0°$ (blue dashed line) and $\alpha = 45°$ (green solid line); (b) time dependence of the fidelity for the atom coupled to the Fock state field. Other parameters used are $n = 0$ and $\Delta = 5\lambda$.

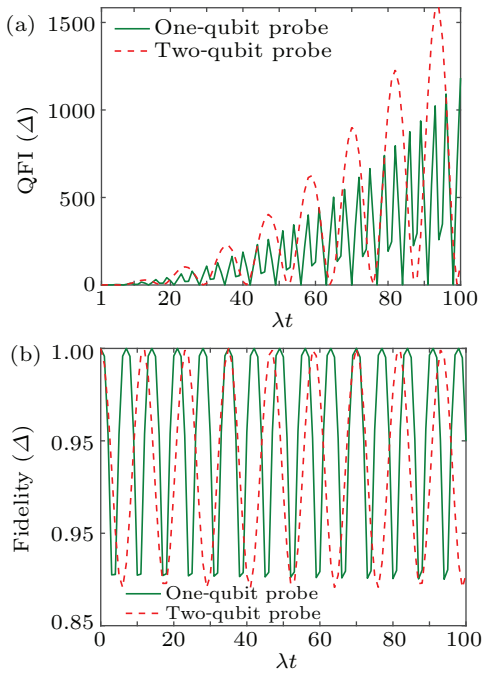


Fig. 2. (a) The QFI of the detuning, (b) time dependence of the fidelity of the atomic system when the atoms interact with the Fock state field for different numbers of atom probes. The green solid lines correspond to the one-qubit probe. The red dashed lines denote the two-qubit probe. The other parameters used as Fig. 1.

The QFI dynamics of the detuning with two-qubit probe is drawn in Fig. 2(a) with red dashed line. The green solid lines, which have been shown in Fig. 1, correspond to the one-qubit probe. Surprisingly, the QFI of the detuning displays the behavior of collapse and revival, which manifests that there is the memory effect. As a whole, the optimal precision of the detuning estimation in each period is enhanced with increasing time. For the detuning estimation with two-qubit probe, the maximal QFI shown in Fig. 2(a) is 1.58×10^3 in the last period. The fidelity of the atomic system is plotted in Fig. 2(b) when the atoms interact with the Fock state field. Figure 2(b) indicates that the fidelity of the atomic system is reduced with the two-qubit probe. From red dashed lines in Fig. 2, one can see that the QFI and the fidelity simultaneously achieve the optimum value at longer times. The reason behind this is that the optimal fidelity stands for the maximal entanglement state of the atomic system, which is useful for the parameter estimation.

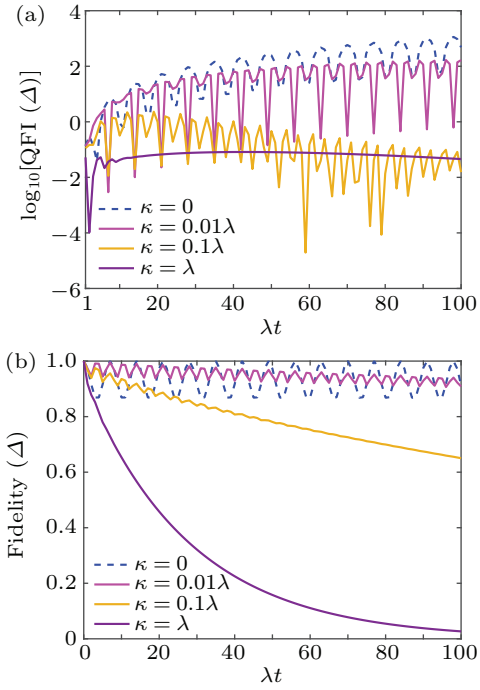


Fig. 3. When one-qubit probe is applied and the cavity decay rate is considered, (a) QFI of the detuning Δ as a function of time for different cavity decay rate κ, $\kappa = 0$ (blue dashed line), $\kappa = 0.01\lambda$ (magenta solid line), $\kappa = 0.1\lambda$ (orange solid line), and $\kappa = \lambda$ (purple solid line); (b) time dependence of the fidelity for the atom coupled to the Fock state field. The initial state of the system is set as $\alpha = 0°$. Other parameters used as Fig. 1.

Now, we investigate the effect of the decay on estimating the detuning. Comparing with the cavity decay rate, the atomic decay rate can be neglected by appropriately choosing the atomic transition.[68] Hence, we only investigate the effect of the cavity decay rate on estimating the detuning. For one-qubit probe, the master equation of the atom–cavity system interacting with the vacuum reservoir is (we adopt $\hbar = 1$)

$$\frac{\partial \rho}{\partial t} = -\mathrm{i}\left[H_{\mathrm{I}}', \rho\right] + \kappa\left(\hat{a}\rho\hat{a}^{\dagger} - \frac{1}{2}\hat{a}^{\dagger}\hat{a}\rho - \frac{1}{2}\rho\hat{a}^{\dagger}\hat{a}\right), \quad (11)$$

where κ is the cavity decay rate. Due to the assumption that the atom–cavity system is prepared initially in the state $|\psi_{(0)}\rangle = \cos(\alpha)|e,0\rangle + \sin(\alpha)|g,1\rangle$, the bases of the system are $|e,0\rangle$, $|g,1\rangle$ and $|g,0\rangle$. By plugging the Hamiltonian and the initial state of system into the above equation and tracing over the cavity field degrees of freedom, we can obtain the reduced density matrix of the atom. Then, the QFI of the detuning and the fidelity of the one-qubit probe are calculated by Eqs. (2) and (4).

When one-qubit probe is applied and the cavity decay rate is considered, the QFI of the detuning and the fidelity of the one-qubit probe as a function of the interaction time are shown in Fig. 3. The results reveal that when the cavity decay rate increases, the QFI and the fidelity decrease, and the oscillatory behavior of the QFI and the fidelity are suppressed. Comparing the result of the lossless (blue dashed line) with that of the low loss (magenta solid line), one can see that the QFI and the fidelity are robust in the low loss.

3.2. The quantum estimation of the temperature in the thermal reservoir

For the purpose of estimating the temperature with a high precision, we assume a single two-level atom interacts with a thermal reservoir. The equation of reduced density matrix evolution of the atom is written as

$$\begin{aligned}\frac{\mathrm{d}\rho}{\mathrm{d}t} &= -\frac{1}{2}\gamma(m+1)[\sigma_+\sigma_-\rho - 2\sigma_-\rho\sigma_+ + \rho\sigma_+\sigma_-] \\ &\quad -\frac{1}{2}\gamma m[\sigma_-\sigma_+\rho - 2\sigma_+\rho\sigma_- + \rho\sigma_-\sigma_+],\end{aligned} \tag{12}$$

where γ is the atomic decay rate, and m is the thermal average boson number, that is, $m = 1/[\exp(\frac{\hbar\nu_k}{k_\mathrm{B}T}) - 1]$. The atomic density matrix elements are obtained as

$$\rho_{11} = \frac{m}{2m+1} + \left[\cos^2(\alpha) - \frac{m}{2m+1}\right]\mathrm{e}^{-\gamma(2m+1)t}, \tag{13a}$$

$$\rho_{12} = \cos(\alpha)\sin(\alpha)\,\mathrm{e}^{-\gamma(m+\frac{1}{2})t}, \tag{13b}$$

$$\rho_{21} = \cos(\alpha)\sin(\alpha)\,\mathrm{e}^{-\gamma(m+\frac{1}{2})t}, \tag{13c}$$

$$\rho_{22} = \frac{m+1}{2m+1} - \left[\cos^2(\alpha) - \frac{m}{2m+1}\right]\mathrm{e}^{-\gamma(2m+1)t}. \tag{13d}$$

When two two-level atoms interact with the thermal reservoir, the evolved state of the system is shown as follows:

$$\rho_3(t) = \begin{pmatrix} \rho_{11} & 0 & 0 & 0 \\ 0 & \rho_{22} & \rho_{23} & 0 \\ 0 & \rho_{32} & \rho_{33} & 0 \\ 0 & 0 & 0 & \rho_{44} \end{pmatrix}, \tag{14}$$

where the elements of the reduced density matrix are expressed as Eq. (A2) of Ref. [69], respectively. Suppose the initial atomic state is the maximal entanglement state, the value of parameter a in the Eq. (A2) of Ref. [69] will be set as $a = 0$. For simplicity, we assume $m = n$, $\gamma_1 = \gamma_2$, $r_1 = r_2$ and $\theta_1 = \theta_2 = 0$.

Afterwards, the QFI of the mean photon number can be given by Eq. (2). Furthermore, the QFI of the temperature can be expressed by the QFI of the mean photon number

$$F_\mathrm{Q}(T) = F_\mathrm{Q}(m)\left(\frac{\partial m}{\partial T}\right)^2, \quad \frac{\partial m}{\partial T} = \frac{\hbar\omega_0\,\mathrm{e}^{\frac{\hbar\omega_0}{k_\mathrm{B}T}}}{(\mathrm{e}^{\frac{\hbar\omega_0}{k_\mathrm{B}T}} - 1)^2 k_\mathrm{B}T^2}. \tag{15}$$

And the fidelity between the initial and final states of the atomic system is obtained in the thermal reservoir.

When the probe is a single qubit, the QFI of the temperature is presented in Fig. 4(a) for different initial atomic states. One can find that the QFI of the temperature is enhanced with the increase of the time when the initial atomic state is the superposition state ($\alpha = 45°$), while the QFI grows quickly at first and then remains constant when the initial atomic state is an eigenstate ($\alpha = 0°$). Time dependence of the fidelity of the atom coupled to a thermal reservoir is plotted in Fig. 4(b), which indicates the fidelity of the initial superposition state is always larger than that of the initial eigenstate. Therefore, the superposition state is the best choice for estimating the temperature with a high precision. And the maximal QFI of the temperature with the one-qubit probe is 80 at $\gamma t = 10$.

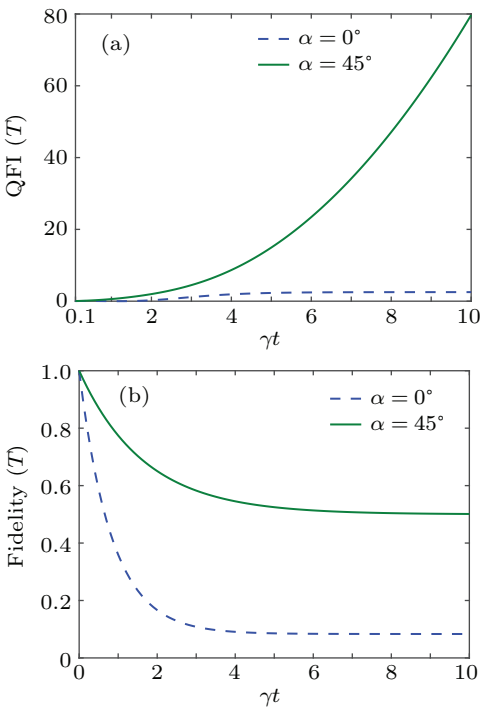


Fig. 4. When one-qubit probe is applied, (a) QFI of the temperature T as a function of time for different α, $\alpha = 0°$ (blue dashed line) and $\alpha = 45°$ (green solid line); (b) time dependence of the fidelity for the atom interacts with a thermal reservoir. Other parameters used are $\hbar\nu_k/k_\mathrm{B} = 1$, $m = 0.1$ and $\gamma = 1$.

For the estimation of the temperature, we make a comparison between the one-qubit and two-qubit probe, as plotted in Fig. 5. When the interaction time increases, the QFI of the temperature with the two-qubit probe reveals an initial increase and then a steady value is shown in Fig. 5(a). The maximal QFI with two-qubit probe is close to 5, which is far less

than the one-qubit probe with the superposition initial state. The fidelity of the atomic system is plotted in Fig. 5(b) when the atoms interact with the thermal reservoir. The green solid lines, which have been shown in Fig. 4, correspond to the one-qubit probe, while the red dashed lines correspond to the two-qubit probe. Figure 5(b) indicates that the fidelity of the atomic system is reduced with the two-qubit probe.

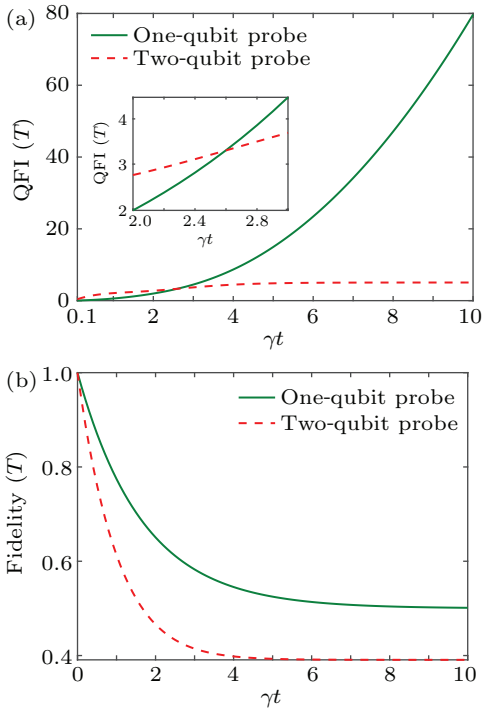


Fig. 5. (a) The QFI of temperature, (b) time dependence of the fidelity of the atomic system when the atoms interact with the thermal reservoir for different numbers of atom probes. The green solid lines correspond to the one-qubit probe. The red dashed lines denote the two-qubit probe. The other parameters used as Fig. 3.

3.3. The quantum estimation of the squeezing strength in the squeezed vacuum reservoir

Now we assume a single two-level atom is immersed in a squeezed vacuum reservoir for estimating the squeezing strength. The equation of motion for the atomic density matrix is written as

$$\begin{aligned}\frac{\mathrm{d}\rho}{\mathrm{d}t} &= -\frac{1}{2}\gamma(M+1)[\sigma_+\sigma_-\rho - 2\sigma_-\rho\sigma_+ + \rho\sigma_+\sigma_-] \\ &\quad -\frac{1}{2}\gamma M[\sigma_-\sigma_+\rho - 2\sigma_+\rho\sigma_- + \rho\sigma_-\sigma_+] \\ &\quad -\gamma \mathrm{e}^{-\mathrm{i}\theta}N\sigma_-\rho\sigma_- - \gamma\mathrm{e}^{\mathrm{i}\theta}N\sigma_+\rho\sigma_+, \end{aligned} \tag{16}$$

where $M=\sinh^2(r)$, $N=\cosh(r)\sinh(r)$, and r is the squeezing strength. θ denotes the reference phase. For simplicity, the reference phase is fixed at $\theta=0$. The equations of motion for the density matrix elements are

$$\dot{\rho}_{11} = \gamma M\rho_{22} - \gamma(M+1)\rho_{11}, \tag{17a}$$

$$\dot{\rho}_{12} = -\gamma\left(M+\frac{1}{2}\right)\rho_{12} - \gamma N\rho_{21}, \tag{17b}$$

$$\dot{\rho}_{21} = -\gamma\left(M+\frac{1}{2}\right)\rho_{21} - \gamma N\rho_{12}, \tag{17c}$$

$$\dot{\rho}_{22} = \gamma(M+1)\rho_{11} - \gamma M\rho_{22}. \tag{17d}$$

Then, the atomic density matrix elements are given by

$$\rho_{11} = \frac{M}{2M+1} + \left[\cos^2(\alpha) - \frac{M}{2M+1}\right]\mathrm{e}^{-\gamma(2M+1)t}, \tag{18a}$$

$$\rho_{12} = \cos(\alpha)\sin(\alpha)\,\mathrm{e}^{-\gamma(M+N+\frac{1}{2})t}, \tag{18b}$$

$$\rho_{21} = \cos(\alpha)\sin(\alpha)\,\mathrm{e}^{-\gamma(M+N+\frac{1}{2})t}, \tag{18c}$$

$$\rho_{22} = \frac{M+1}{2M+1} - \left[\cos^2(\alpha) - \frac{M}{2M+1}\right]\mathrm{e}^{-\gamma(2M+1)t}. \tag{18d}$$

When two two-level atoms interact with the squeezed vacuum reservoir, the evolved state of the system is shown as follows:

$$\rho_4(t) = \begin{pmatrix} \rho_{11} & 0 & 0 & \rho_{14} \\ 0 & \rho_{22} & \rho_{23} & 0 \\ 0 & \rho_{32} & \rho_{33} & 0 \\ \rho_{41} & 0 & 0 & \rho_{44} \end{pmatrix}, \tag{19}$$

where the elements of the reduced density matrix are expressed as Eq. (B2) of Ref. [69], respectively.

The QFI of the squeezing strength is obtained by Eqs. (2), (18) and (19). When the atomic probe is employed, the fidelity of the atomic system embedded in the squeezed vacuum reservoir can be calculated by using Eqs. (3), (18) and (19).

When the probe is a single qubit, the QFI of the squeezing strength as a function of dimensionless time γt is shown in Fig. 6(a). From Fig. 6(a), one can find the increase of the interaction time is beneficial to estimating the squeezing strength. When $\alpha=0°$, a drop and rise of the QFI occurs at $\gamma t\simeq 1.20$. It is caused by the following reasons: one is that the process of the information of the squeezing strength is encoded into the atom, and the other is the decoherence effect. If the decoherence effect is greater than the process of the information of the squeezing strength encoded into the probe, the estimation precision of the squeezing strength will decrease, otherwise, the estimation precision of the squeezing strength will increase. Time dependence of the fidelity for the atom immersed into a squeezed vacuum reservoir is exhibited in Fig. 6(b). Figure 6(b) shows the final atomic state is completely different from the initial atomic state when $\alpha=0°$. Comparing Figs. 6(a) and 6(b), we find that superposition states can improve the estimation precision of the squeezing strength. The estimation of the squeezing strength shows the similarity with the case of the temperature estimation. The maximal QFI of the squeezing strength with the one-qubit probe is 5.41×10^2 at $\gamma t=10$.

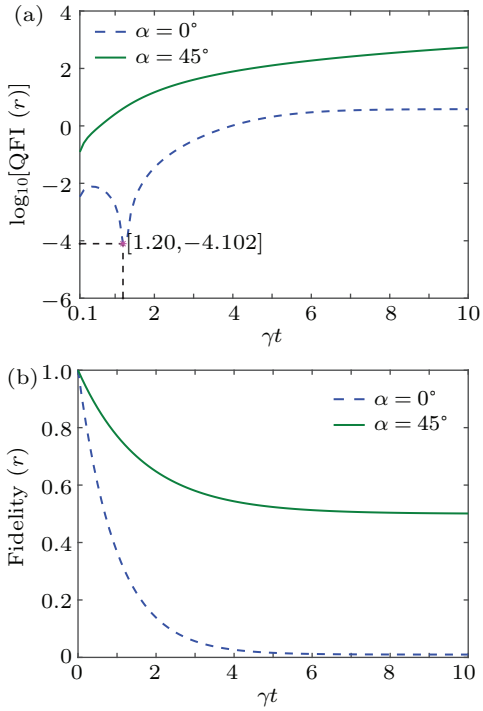


Fig. 6. When one-qubit probe is applied, (a) QFI of the squeezing strength r as a function of time for different α, $\alpha = 0°$ (blue dashed line) and $\alpha = 45°$ (green solid line); (b) time dependence of the fidelity for the atom interacts with a squeezed vacuum reservoir. Other parameters used are $\theta = 0$, $r = 0.1$ and $\gamma = 1$.

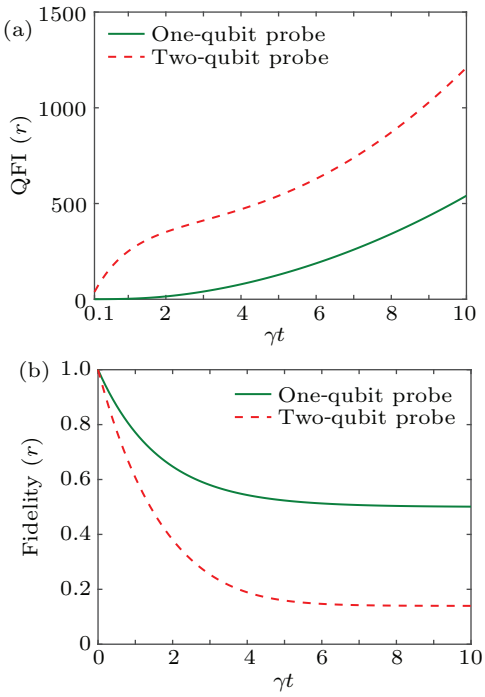


Fig. 7. (a) The QFI of the squeezing strength, (b) time dependence of the fidelity of the atomic system when the atoms interact with the squeeze vacuum reservoir for different numbers of atom probes. The green solid lines correspond to the one-qubit probe. The red dashed lines denote the two-qubit probe. The other parameters used as Fig. 5.

Figure 7(a) presents the QFI of the squeezing strength with the two-qubit probe increases monotonically in time, and up to the value 1.21×10^3 at $\gamma t = 10$. The fidelity of the atomic system is plotted in Fig. 7(b) when the atoms interact with the squeezed vacuum reservoir. The green solid lines, which have been shown in Fig. 6, correspond to the one-qubit probe, while the red dashed lines correspond to the two-qubit probe. For estimating the squeezing strength, the QFI with the one-qubit probe is close to 0 within the high probe fidelity, which is far less than the QFI with the two-qubit probe. Figure 7 tells us that only the precision of the parameter estimation is optimal with the two-qubit probe.

4. Conclusions

In this paper, a simple and feasible scheme approach is presented to estimate the environmental parameter, the detuning, the temperature of the thermal reservoir and the squeezing strength of the squeezed vacuum reservoir. When the detuning between the atomic transition frequency and the frequency of the cavity field is estimated, there is the memory effect. Besides, we find the precision of estimation is evidently enhanced by utilizing two-qubit probe. For the temperature estimation, when the probe is a single qubit with the superposition initial state, the estimation precision monotonously increases with the increase of the interaction time. The results show that both the precision of the parameter estimation and the fidelity of the atomic system are optimal with the initially superposition state of the one-qubit probe. When the squeezing strength of the squeezed vacuum reservoir is estimated, the dynamics of the QFI appears a drop and rise by using the one-qubit probe with the initial eigenstate. Although the precision of the squeezing strength estimation is improved by using the two-qubit probe, the fidelity of the atomic system is reduced by comparing with the one-qubit probe. Based on the quantum Cramér–Rao bound, the estimation precision of parameters can be obtained. In the time range, $0 < \lambda t \leq 100$ and $0 < \gamma t \leq 10$, the maximal QFI of the estimated parameters are 1.58×10^3, 80 and 1.21×10^3, respectively. And the precision of estimated parameters can be further improved via increasing the interaction time. The reason behind this result is that the measurement of the detuning, the temperature and the squeezing strength corresponds to the measurement of the energy, and from the energy-time uncertainty relation $\Delta E \cdot \Delta t \geq \hbar$,[70] the realization of the limit $\Delta E \to 0$ requires the time $\Delta t \to \infty$.

Our work not only shows the sudden drop of the QFI can be suppressed at longer time in the dissipation environment, but also provides the optimized probe state for achieving the ultimate bound of parameter estimation in open quantum systems. In addition, the initial atomic state and configuration in our scheme are easy enough to implement in practice compared with that in previous studies, such as the GHZ state,[39] the pure dephasing of the probes,[47] and time-local optimal control.[61] One possible future goal is to simultaneously improve the estimation precision of the environmental parameter and the fidelity of the atom probe by optimizing the model or

measurement method.[71] Our results provide a potential application in the laser frequency stabilization technique, quantum thermometry, and quantum metrology.

Acknowledgements

Project supported by the National Natural Science Foundation of China (Grant Nos. 91536115 and 11534008) and Natural Science Foundation of Shaanxi Province, China (Grant No. 2016JM1005).

References

[1] Geononi M G, Olivares S and Paris M G A 2011 *Phys. Rev. Lett.* **106** 153603
[2] Demkowicz-Dobrzański R 2011 *Phys. Rev. A* **83** 061802(R)
[3] Chwedeńczuk J, Piazza F and Smerzi A 2011 *New J. Phys.* **13** 065023
[4] Pinel O, Jian P, Treps N, Fabre C and Braun A D 2013 *Phys. Rev. A* **88** 040102(R)
[5] Zhang L J and Xiao M 2013 *Chin. Phys. B* **22** 110310
[6] Xiang G Y and Guo G C 2013 *Chin. Phys. B* **22** 110601
[7] Yao Y, Ge L, Xiao X, Wang X G and Sun C P 2014 *Phys. Rev. A* **90** 022327
[8] He Z and Yao C M 2014 *Chin. Phys. B* **23** 110601
[9] Li Y L, Xiao X and Yao Y 2015 *Phys. Rev. A* **91** 052105
[10] Chapeau-Blondeau F 2015 *Phys. Rev. A* **91** 052310
[11] Berni A A, Gehring T, Nielsen B M, Händchen V, Paris M G A and Andersen U L 2015 *Nat. Photon.* **9** 577
[12] Gillard N, Belin E and Chapeau-Blondeau F 2017 *Phys. Lett. A* **381** 2621
[13] Metwally N and Hassan S S 2017 *Laser Phys. Lett.* **14** 115204
[14] Gagatsos C N, Bash B A, Guha S and Datta A 2017 *Phys. Rev. A* **96** 062306
[15] Yang Y, Liu X B, Wang J C and Jing J L 2018 *Quantum. Inf. Process.* **17** 54
[16] Yu X, Zhao X, Shen L Y, Shao Y Y, Liu J and Wang X G 2018 *Opt. Express* **26** 16292
[17] Jing X X, Liu J, Xiong H N and Wang X G 2015 *Phys. Rev. A* **92** 012312
[18] Berrada K 2016 *Quantum. Inf. Process.* **15** 4897
[19] Górecka A, Pollock F A, Liuzzo-Scorpo P, Nichols R, Adesso G and Modi K 2018 *New J. Phys.* **20** 083008
[20] Feng X N and Wei L F 2017 *Sci. Rep.* **7** 15492
[21] Pezzé L and Smerzi A 2009 *Phys. Rev. Lett.* **102** 100401
[22] Ren Z H, Li Y, Li Y N and Li W D 2019 *Acta. Phys. Sin.* **68** 040601 (in Chinese)
[23] Taylor M A and Bowen W P 2016 *Phys. Rep.* **615** 1
[24] Giowannetti V, Lloyd S and Maccone L 2006 *Phys. Rev. Lett.* **96** 010401
[25] Demkowicz-Dobrzański R and Maccone L 2014 *Phys. Rev. Lett.* **113** 250801
[26] Huelga S F, Macchiavello C, Pellizzari T, Ekert A K, Plenio M B and Cirac J I 1997 *Phys. Rev. Lett.* **79** 3865
[27] Kacprowicz M, Demkowicz-Dobrzański R, Wasilewski W, Banaszek K and Walmsley I A 2010 *Nat. Photon.* **4** 357
[28] Chaves R, Brask J B, Markiewicz M, Kołodyński J and Acín A 2013 *Phys. Rev. Lett.* **111** 120401
[29] Dinani H T and Berry D W 2014 *Phys. Rev. A* **90** 023856
[30] Hyllus P, Gühne O and Smerzi A 2010 *Phys. Rev. A* **82** 012337
[31] Sahota J and Quesada N 2015 *Phys. Rev. A* **91** 013808
[32] Huang J, Guo Y N and Xie Q 2016 *Chin. Phys. B* **25** 020303
[33] Yan K, Xie Y Q, Huang Y M and Hao X 2017 *Commun. Theor. Phys.* **67** 261
[34] Lin D P, Liu Y and Zou H M 2018 *Chin. Phys. B* **27** 110303
[35] Ji Y H, Ke Q and Hu J J 2020 *Chin. Phys. B* **29** 120303
[36] Gammelmark S and Mølmer K 2014 *Phys. Rev. Lett.* **112** 170401
[37] Kiilerich A H and Mølmer K 2015 *Phys. Rev. A* **91** 012119
[38] Dinani H T, Gupta M K, Dowling J P and Berry D W 2016 *Phys. Rev. A* **93** 063804
[39] Mogilevtsev D, Garusov E, Korolkov M V, Shatokhin V N and Cavalcanti S B 2018 *Phys. Rev. A* **98** 042116
[40] Guo L S, Xu B M, Zou J and Shao B 2015 *Phys. Rev. A* **92** 052112
[41] Farajollahi B, Jafarzadeh M, Rangani Jahromi H and Amniat-Talab M 2018 *Quantum. Inf. Process.* **17** 119
[42] Zhao Z X, Pan Q Y and Jing J L 2020 *Phys. Rev. D* **101** 056014
[43] Xie D, Xu C L and Wang A M 2017 *Quantum. Inf. Process.* **16** 155
[44] Razavian S, Benedetti C, Bina M, Akbari-Kourbolagh Y and Paris M G A 2019 *Eur. Phys. J. Plus* **134** 284
[45] Zhu W L, Wu W and Luo H G 2020 *Chin. Phys. B* **29** 020501
[46] Rangani Jahromi H 2020 *Phys. Scr.* **95** 035107
[47] Gebbia F, Benedetti C, Benatti F, Floreanini R, Bina M and Paris M G A 2020 *Phys. Rev. A* **101** 032112
[48] Srikanth R and Banerjee S 2008 *Phys. Rev. A* **77** 012318
[49] Anisimov P M, Raterman G M, Chiruvelli A, Plick W N, Huver S D, Lee H and Dowling J P 2010 *Phys. Rev. Lett.* **104** 103602
[50] Zhang X X, Yang Y X and Wang X B 2013 *Phys. Rev. A* **88** 013838
[51] Szigeti S S, Tonekaboni B, Lau W Y S, Hood S N and Haine S A 2014 *Phys. Rev. A* **90** 063630
[52] Wu S X, Yu C S and Song H S 2015 *Phys. Lett. A* **379** 1228
[53] Liu P, Wang P, Yang W, Jin G R and Sun C P 2017 *Phys. Rev. A* **95** 023824
[54] Milburn G J, Chen W Y and Jones K R 1994 *Phys. Rev. A* **50** 801
[55] Chiribella G, D'Ariano G M and Sacchi M F 2006 *Phys. Rev. A* **73** 062103
[56] Gaiba R and Paris M G A 2009 *Phys. Lett. A* **373** 934
[57] Genoni M G, Invernizzi C and Paris M G A 2009 *Phys. Rev. A* **80** 033842
[58] Šafránek D, Lee A R and Fuentes I 2015 *New J. Phys.* **17** 073016
[59] Šafránek D and Fuentes I 2016 *Phys. Rev. A* **94** 062313
[60] Rigovacca L, Farace A, Souza L, De Pasquale A, Giovannetti V and Adesso G 2017 *Phys. Rev. A* **95** 052331
[61] Predko A, Albarelli F and Serafini A 2020 *Phys. Lett. A* **384** 126268
[62] Purcell E M, Bloembergen N and Pound R V 1946 *Phys. Rev.* **70** 988
[63] Helstron C W 1976 *Quantum Detection and Estimation Theory* (New York: Academic Press)
[64] Holevo A S 1982 *Probabilistic and statistical aspects of quantum theory* (Amsterdam: North Holland)
[65] Zhong W, Sun Z, Ma J, Wang X G and Nori F 2013 *Phys. Rev. A* **87** 022337
[66] Jozsa R 1994 *J. Mod. Opt.* **41** 2315
[67] Scully M O and Zubairy M S 1997 *Quantum Optics* (Cambridge: Cambridge University Press)
[68] Zhu C J, Ping L L, Yang Y P and Agarwal G S 2020 *Phys. Rev. Lett.* **124** 073602
[69] Ikram M, Li F L and Zubairy M S 2007 *Phys. Rev. A* **75** 062336
[70] Aharonov Y, Massar S and Popescu S 2002 *Phys. Rev. A* **66** 052107
[71] Liao X P, Fang M F and Zhou X 2017 *Quantum. Inf. Process.* **16** 241